Analytica Chimica Acta 712 (2012) 120–126

Contents lists available at SciVerse ScienceDirect

Analytica Chimica Acta

journal homepage: www.elsevier.com/locate/aca

Mn-doped ZnS quantum dots for the determination of acetone by phosphorescence attenuation

Emma Sotelo-Gonzalez, María T. Fernandez-Argüelles, Jose M. Costa-Fernandez, Alfredo Sanz-Medel*

Department of Physical and Analytical Chemistry, University of Oviedo, Avda. Julian Claveria 8, E-33006 Oviedo, Spain

ARTICLE INFO

Article history:
Received 29 June 2011
Received in revised form 7 November 2011
Accepted 8 November 2011
Available online 19 November 2011

Keywords:
Quantum dots
Phosphorescence
Luminescence
Acetone determination
Nanoparticles

ABSTRACT

Quantum dot (QD) nanoparticles (NPs) are increasingly used as highly valuable fluorescent biomarkers and as sensitive (bio)chemical probes. Interestingly, if certain metal impurities are incorporated during the NPs synthesis, phosphorescent QDs with analytical potential can be obtained.

We report here the synthesis of colloidal manganese-doped ZnS nanoparticles which have been surface-modified with L-cysteine that exhibit an intense room temperature phosphorescence (RTP) emission in aqueous media even in the presence of dissolved oxygen (i.e. sample deoxygenation is not needed). An exhaustive RTP photoluminescent and morphological characterization of the synthesized QDs and their potential for development of phosphorescent analytical methodologies is described. Application to analytical control of acetone ("model analyte" from the ketones family) in water and urine samples is carried out by measuring the QDs phosphorescence quenching rate.

The observed results showed a high selectivity of Mn^{2+}-doped ZnS QDs towards acetone. The linear range of the developed methodology turned out to be at least up to 600 mg L^{-1} with a detection limit (DL) for acetone dissolved in aqueous medium of 0.2 mg L^{-1}. The developed methodology was finally applied for acetone determination in different spiked water and urine samples, and the recoveries fall in the range of 93–107%.

© 2011 Elsevier B.V. All rights reserved.

1. Introduction

Acetone is a solvent widely used in various industrial processes particularly in manufacturing strengthened plastic fibres and shoes. The presence of acetone in the environment results from different sources such as sewage disposal, industrial leaching or emissions from automobiles or turbines [1] and their toxic effects on the human organisms are known for a long time [2]. Interest in acetone determination in waters, along with many other low molecular weight carbonyl compounds, have increased in recent years owing to the wide variety of its sources, the risk of contamination by acetone and its potential adverse health effects in drinking water [3,4]. In surface waters, the presence of such compounds was also ascribed to the photodegradation of dissolved organic matter and to microbial processes [5]. Moreover, detection of acetone levels in urine (known as ketonuria) and blood (known as diabetic ketoacidosis) can be used as a potential biomarker for diagnosis of some diseases such as Diabetes Mellitus or starving [6–8].

The vast majority of analytical methods used for acetone determination are based on chromatographic techniques. Frequently, such methods require complex and long-lasting sample pretreatment steps (e.g. solid-phase microextraction, sample derivatizations, etc.). Additionally, photoluminescence approaches for sensitive acetone detection using organic molecules as photoluminescent probes are common today. In this vein, in the last few years improvements in nanotechnology allowed replacement of conventional organic fluorophores by alternative advantageous luminescent nanomaterials such as quantum dots which have recently demonstrated their high potential in the development of novel luminescent bioanalytical methodologies [9–12].

Quantum dots (QDs) are nanocrystals of semiconductor materials with particle sizes between 2 and 10 nm exhibiting unexpected optical and electronic properties [13]. Quantum confinement effects are responsible for such remarkable properties, which depend on their size and composition. Such effects offer the analyst high fluorescent quantum yields, narrow and symmetric size-tuneable emission spectra, high resistance to photobleaching and long fluorescence lifetimes, features which can be highly useful in luminescence based analysis [14–16].

Luminescence of quantum dots is very sensitive to their surface states. Therefore, eventual chemical or physical interactions between a given chemical species with the surface of the nanoparticles could result in changes of the efficiency of the core electron–hole recombination [17]. This was the basis of the recent increasing research activity on the development of novel analytical

* Corresponding author. Tel.: +34 985103474; fax: +34 985103474.
E-mail addresses: jcostafe@uniovi.es (J.M. Costa-Fernandez), asm@uniovi.es (A. Sanz-Medel).

0003-2670/$ – see front matter © 2011 Elsevier B.V. All rights reserved.
doi:10.1016/j.aca.2011.11.023

methodologies based on QDs for direct analysis of small molecules and ions [9,18]. Methods based on direct chemical or physical interactions between target chemical species (analyte) and the surface of the nanoparticles are very simple and have demonstrated high sensitivity features. Unfortunately, very often those methods lack of an appropriate selectivity.

To improve selectivity of QDs based sensors, elimination of interferences from other concomitant fluorescent compounds emissions is a must. Recent investigations have evaluated the use of metallic dopants with quantum states remote from the valence and conduction band edges of the semiconductor nanoparticles to generate different radiative processes [19,20]. In this vein, Mn^{2+}-doped ZnS QDs have attracted considerable attention lately because doping Mn^{2+} ions may act as recombination centres for the excited electron–hole pairs and result in strong and characteristic luminescence at longer wavelengths. Upon Mn^{2+} doping, a characteristic emission band centred at around 590 nm, is developed for the well-known $^4T_1$–$^6A_1$ d–d transition of Mn^{2+} ions on Zn^{2+} sites of the QD (where Mn^{2+} is coordinated by S^{2-}) [21–23]. When compared with traditional QDs such as CdSe or ZnS, the resulting Mn^{2+}-doped ZnS QDs exhibit both, longer Stokes shift between excitation and emission wavelengths and longer luminescent lifetimes (in the order of a few ms), properties which are typical from phosphorescent emission [24]. Hence, it is possible to perform time resolved measurements allowing simple discrimination between the luminescence emission from Mn:ZnS QDs from the background fluorescence of the sample (in which luminescent lifetime is shorter). Additionally, when compared to the commonly used CdSe or CdS QDs, the absence of Cd^{2+} in Mn^{2+}-doped ZnS quantum dots can minimize toxicity of such nanocrystals (particularly important in live-experiments) due to the eventual release of such toxic metal ions from the nanocrystals. These advantages make Mn^{2+}-doped ZnS QDs very exciting advanced nanomaterials as analytical luminescent labelling agents for imaging and sensing.

In this context, in a pioneer work, surface-modified Mn^{2+}-doped ZnS QDs were used for direct sensing of the antibiotic enoxacin in biological fluids based on quenching of the phosphorescence emission of the nanoparticles [25]. More recently, enhancement of the phosphorescence emission of Mn:ZnS QDs in presence of ascorbic acid was used for the determination of such essential nutritional factor. For this purpose, QDs were coated with sodium tripolyphosphate, which forms a chelate with ascorbic acid. Authors proposed that the chelate formed extracted Mn and Zn from the surface of the QDs, generating more holes and allowing the reduction of Mn^{3+} to Mn^{2+}, enhancing the emission of the QDs [26]. The same Mn:ZnS QDs were conjugated to glucose oxidase (GOD) to carry out an enzymatic determination of glucose. In this approach, the presence of glucose generated the formation of H_2O_2, which is an effective quencher of the phosphorescence of Mn:ZnS [27]. Very recently, the use of Mn-doped QDs have been proposed for the development of multidimensional sensing devices for discrimination of proteins based on measurements of fluorescence, phosphorescence and light scattering. Values of these three parameters were obtained for eight different proteins after interaction with the QDs, and a fingerprint pattern was obtained after a Principal Component Analysis [28].

In this paper, colloidal Mn^{2+}-doped ZnS nanoparticles exhibiting room temperature phosphorescence (RTP) emission have been synthesized and water solubilized by capping the QDs surface with L-cysteine. Such coating of the nanoparticle with cysteine groups did not affect their emission properties, allowing their analytical application for acetone determination (selected as model ketone specie) in aqueous media by measuring the quenching on the RTP emission of such QDs after direct interaction with the analyte.

2. Experimental

2.1. Reagents

All chemical reagents used were of analytical-reagent grade and used as received, without any further purification. De-ionized Milli-Q water was employed in the preparation of all solutions.

Zinc sulfate heptahydrate, manganese chloride tetrahydrate, L-cysteine hydrochloride monohydrate, potassium bromide, potassium iodide, sodium sulfite, 2-propanol and standard solutions of different cations (Ag^+, Na^+, K^+, Ca^{2+}, Cd^{2+}, Cu^{2+}, Hg^{2+}, Pb^{2+}, Mg^{2+}, Mn^{2+}, Zn^{2+}, and Fe^{3+}) were obtained from MERK (Darmstadt, Germany). Sodium sulfide nonahydrate, D-glucose, Triton X-100, hexadecyltrimethylammonium-bromide (CTAB), trimethyl(tetradecyl)ammonium bromide, sodiumdodecyl sulfate (SDS), sodium hydroxide, acetone solution (2000 $\mu g\,mL^{-1}$ in methanol:water (9:1) and 5000 $\mu g\,mL^{-1}$ in methanol:water (9:1)) and methanol HPLC gradient grade was purchased from Sigma–Aldrich (Milwaukee, WI, USA). Urea and DL-histidine were from Fluka (Basel, Switzerland). Acetone and acetonitrile HPLC gradient grade were purchased from Prolabo (Leuven, Belgium).

2.2. Instrumentation

Phosphorescence and fluorescence spectra were performed on a PerkinElmer LS-50B luminescence spectrometer and Varian Cary Eclipse fluorescence spectrometer (Madrid, Spain), both equipped with xenon discharge lamps. For these measurements, diluted aqueous solutions of QDs were placed in 1 cm quartz cuvettes and their corresponding luminescence was measured. The morphology and microstructure of the QDs were characterized with a transmission electron microscope (TEM) 2000 EXII, JEOL (Tokyo, Japan) and an atomic force microscope (AFM) (Nanotec Electronics, Madrid). FT-IR spectra were collected in a Varian 670 IR FT-IR spectrometer using attenuate total reflectance measurements. Z-potential was measured using a Zetasizer NanoZS (Malvern Instruments Ltd., Worcestershire, United Kingdom) using colloidal QDs in acid medium. All measurements were made at room temperature and atmospheric pressure.

2.3. Synthesis of aqueous ZnS and Mn^{2+}-doped ZnS quantum dots

Colloidal water-soluble ZnS and Mn^{2+}-doped ZnS quantum dots were synthesized in our laboratory via the procedure described by He et al. [25] with some slight modifications. Briefly, 50 mL of 0.02 M L-cysteine, 5 mL of 0.1 M $ZnSO_4$, and 0.15 mL of 0.1 M $MnCl_2$ were mixed in a beaker and pH was adjusted with NaOH 1 M to pH 11. The solution was placed in a three-necked flask and deoxygenated in an argon atmosphere under continuous stirring for 30 min. Then, 5 mL of 0.1 M Na_2S were swiftly injected into the solution to allow the nucleation of the nanoparticles. The mixture was stirred for 20 min, and then the solution was aged at 50 °C under air for 2 h to improve the crystalline structure of the L-cysteine capped Mn^{2+}-doped ZnS QDs. Similarly, ZnS QDs were synthesized using the same procedure but without the addition of $MnCl_2$. Purification of the QDs was carried out by precipitation of the nanoparticles with ethanol in a centrifuge at 5000 rpm for 5 min (the procedure was repeated for 3 times). Finally, the QDs were dried under vacuum and stored under inert argon atmosphere as a water soluble brown solid powder.

2.4. Analytical procedure for acetone measurement

The following general procedures were used to evaluate the effect of the presence of acetone in the nanoparticles environment over luminescence emission of the synthesized phosphorescent QDs.

The optimization studies and calibration curves for acetone determination were obtained by adding increasing amounts of standard water solution of acetone over colloidal suspension of Mn:ZnS QDs in a buffer solution. Once mixed, luminescence emission measurements were performed.

In a similar way, in order to evaluate the effect of potential interfering species on the luminescence emission of Mn^{2+}-doped ZnS QDs, increasing amounts of the assayed chemical species were added over quantum dots buffered solution, and then, QDs phosphorescence emission was measured.

For real sample analysis a simple pre-treatment was used, consisting on a filtration of the samples through 0.45 μm and 0.22 μm filter devices consecutively. Real water samples were prepared by mixing 9 mL of spiked water samples with 1 mL of the synthesized water soluble Mn:ZnS QDs solution at pH 12. Additionally, urine samples were prepared by mixing 1 mL of spiked urine samples with 3 mL of water soluble Mn:ZnS QDs solution at pH 12. Then, the luminescence measurements were performed.

3. Results and discussion

3.1. Characterization of Mn^{2+}-doped ZnS QDs

3.1.1. Morphological characterization of Mn:ZnS QDs

Size characterization was carried out measuring the diameter of the nanocrystal core by transmission electron microscopy (TEM) and atomic force microscopy (AFM). Images obtained by TEM (see Fig. 1) show Mn^{2+}-doped ZnS QDs having nearly spherical shape and almost uniform core size in diameter (about 4 nm).

Conversely, images obtained by atomic force microscopy (AFM) also showed the presence of bigger nanoparticles, with diameters of around 20 nm (see Fig. 2). Such larger particles can be attributed to a partial aggregation of several colloidal nanoparticles that might occur during the sample preparation procedure carried out for AFM measurements (e.g. during the drying process required previous to the AFM analysis). Images from AFM showed also a second population of nanocrystals with lower particle size of about 5 nm (see Fig. 2b). Such low-sized QDs would correspond to single nanocrystals of Mn:ZnS (not aggregated).

In addition, Fourier transform infrared spectroscopy was carried out in order to confirm the bonding of L-cysteine to the nanoparticle surface and to assess the orientation of such L-cysteine ligands surrounding the nanocrystal core. Results showed that the stretching band of the SH thiol group, which can be observed when measuring L-cysteine at around 2540 cm^{-1} (wυ S–H), is not observed when the nanoparticles are evaluated. However, the characteristic band for $-COO^-$ (~1403 cm^{-1}, mυ COO^-) and –COOH (1750 cm^{-1}, υ C=O shift to 1570 cm^{-1} as reported by Chen et al. [29]) are still detected in the FT-IR spectra from the L-cysteine stabilized QDs. Thus, we can conclude that the L-cysteine ligands are bound to the nanocrystal surface through the thiol group, leaving the amino and carboxylate functional groups to the outer part of the shell. This is in agreement with previous findings, using CdSe/ZnS QDs, demonstrating that QDs covered with Zn-containing shells exhibit high affinity to thiol groups from molecules used to solubilize the nanoparticles [30].

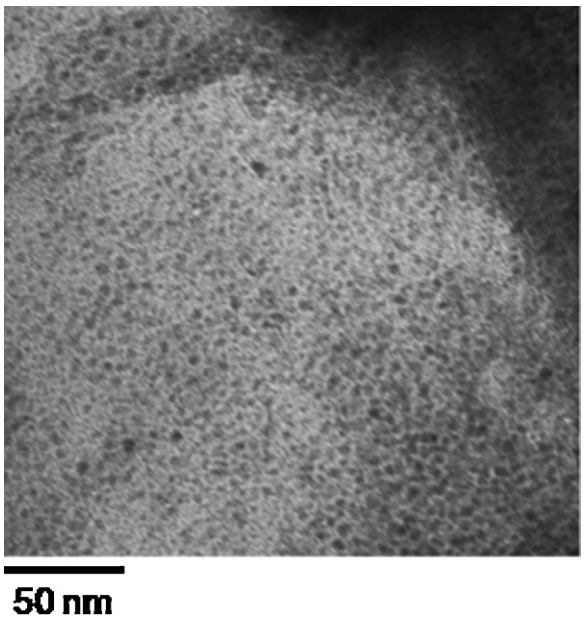

Fig. 1. TEM image of an aqueous solution of the colloidal Mn:ZnS QDs here synthesized.

3.1.2. Spectral characteristics of Mn:ZnS QDs

The synthesized QDs were dispersed in sodium borate buffer (SBB) pH 12. Photoluminescent measurements were carried out at optimized phosphorescence instrumental conditions, with a delay time of 0.04 ms and a gate time of 2 ms. As shown in Fig. 3a, no phosphorescent emission was observed when studying QDs of ZnS without Mn^{2+}. However, when such nanocrystals are doped with Mn^{2+} (solid line in Fig. 3a) an intense emission band centred at around 595 nm, which is attributed to the $^4T_1$–$^6A_1$ prohibited transition, is apparent. Studies showed that no residual fluorescence at 420 nm, typical from the ZnS core QDs [31], was observed, indicating that the doping process of the QDs with Mn^{2+} was highly efficient and no ZnS cores without Mn^{2+} ions seem to exist. Experimental RTP measurement conditions, such as excitation and emission wavelengths at 290 and 595 nm, respectively, were selected for further experiments.

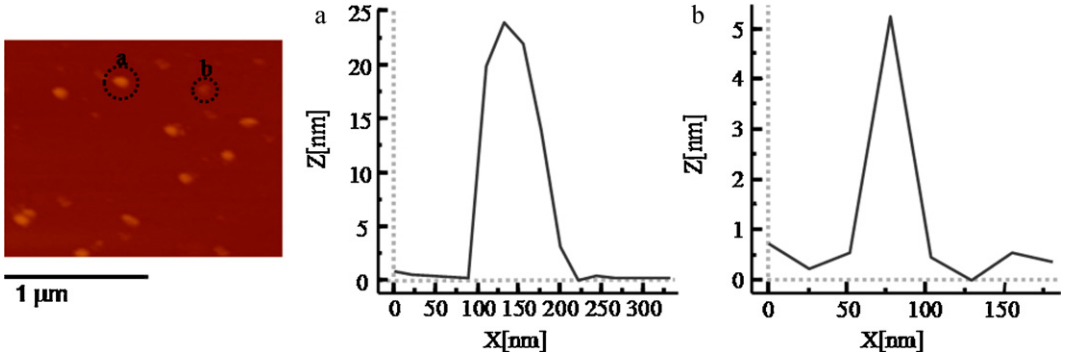

Fig. 2. Topographical AFM image of Mn:ZnS QDs deposited onto a silica surface. Two populations of Mn:ZnS QDs, exhibiting different size-profiles, were obtained.

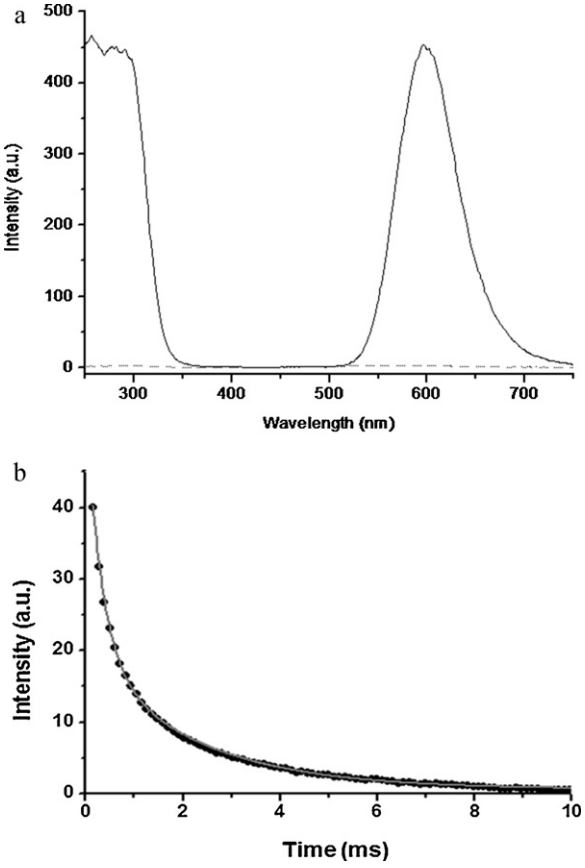

Fig. 3. (a) Excitation and emission spectra of colloidal Mn:ZnS QDs (solid-line) and of colloidal ZnS QDs (dotted line) and (b) Decay curve of luminescence emission of colloidal Mn:ZnS QDs. Emission spectra were obtained by excitation at 290 nm of aqueous solutions of QDs.

Moreover, lifetime measurements of Mn doped ZnS QDs were also carried out and obtained results are shown in Fig. 3b. After excitation by short pulse, the excited state of the QD typically decays following a double exponential time course, with a first lifetime component in the range of 0.3 ms and a second longer lifetime component around 2.1 ms. Such lifetime is very long when compared to ZnS QDs, which present a lifetime on the order of the nanoseconds.

3.1.3. Effect of Mn^{2+} stoichiometry on phosphorescence emission signals

It is well known by now that Mn^{2+} stoichiometry could affect both phosphorescence and fluorescence emission of Mn^{2+}-doped ZnS QDs [32]. In order to investigate nanocrystals composition exhibiting optimum phosphorescence emission characteristics, QDs doped with different Mn:ZnS ratios, ranging 0.3–30 (mol% relative to Zn^{2+}) were synthesized. Photoluminescent studies showed that as the amount of Mn^{2+} increased, the fluorescence emission observed at 420 nm (characteristic from the ZnS core) was lower, and the phosphorescent signal registered was higher. At Mn^{2+} concentrations over a 3% a plateau in the phosphorescent signal was observed. Additionally, measured phosphorescence decay times showed that whereas τ_1 remained constant, τ_2 decreased slightly with increasing concentration of Mn^{2+}. Therefore, Mn^{2+} doped ZnS QDs used for further experiments were selected ensuring 3% Mn^{2+} (relative to Zn^{2+}) in the precursors mixture.

3.1.4. Effect of experimental conditions

In general terms, prediction of the effect of the environment and/or surface functionalization on the optical properties of QDs is difficult. Some parameters of the microenvironment, such as matrix polarity and proticity (hydrogen bonding ability), viscosity, pH along with the presence of surfactants or fluorescence quenchers (e.g. oxygen) can have a strong influence on luminescence intensity [15]. Furthermore, traditional phosphorescence emission is also affected by several parameters, including presence of oxygen, organized media (by adding surfactants) or heavy atoms. Therefore, the eventual effect of all those factors on the RTP emission intensity from Mn^{2+}-doped ZnS QDs was investigated.

Evaluation of pH effect was performed by dissolving the nanoparticles in different buffers of pHs values of: 5, 7.4, 9 and 12. Results showed that pHs between 5 and 9 barely show a difference on the phosphorescence emission, while NPs dispersed in pH 12 buffer showed a substantial increase on the phosphorescence recorded. This could be attributed to the deprotonation of the amino group (p*K*a 10.25) of the L-cysteine nanoparticles layer.

It is well known that dissolved molecular oxygen is a strong quencher of the molecular phosphorescence emission in liquid solutions. Hence, emission of Mn^{2+}-doped QDs was evaluated under different oxygen concentrations by addition of different concentrations of sodium sulphite (up to 20 mM), a well known and effective oxygen scavenger [33]. Unexpectedly, no significant change on the RTP intensity or in luminescence lifetimes from Mn:ZnS QDs (in presence or absence of dissolved oxygen) was observed. This is of course an advantageous feature when compared to traditional phosphorescence emission where removal of oxygen is mandatory [34].

Another critical parameter playing an important role in traditional phosphorescence analytical methods is the presence of heavy atoms in the medium to favor the population of the triplet excited state. Although the transition here is of different nature to those typical triplet–singlet transitions that take place in organic reagents used for RTP, the effect of the presence of high concentration of a heavy atom, including Br and I containing salts (1.2 M) in aqueous media, on the luminescence emission from Mn:ZnS QDs solution was also evaluated. We did not observe any significant variation on the luminescence emission or lifetimes from the Mn^{2+} doped QDs. In fact, the highest values were those obtained for the Mn:ZnS QDs dispersions without presence of such high concentration of salts (which could affect the colloidal stability of the nanoparticles or produce quenching of RTP).

As compared to conventional phosphorescent molecules, the emission of the here-synthesized QDs is highly insensitive to different parameters that typically affect significantly the phosphorescence from the organic molecules. This observed characteristic could be attributed to the difference between the discrete energy levels characteristic of the QDs and those molecular energy levels of conventional organic phosphorescent molecules. Hence, factors that typically affect to transitions of organic molecules do not necessarily affect to transitions that occurs during the emission of QDs.

Finally, since an organized medium is known to enhance the probability of RTP to occur, the effect on RTP of the addition to colloidal Mn:ZnS QDs aqueous solution of surfactants of different nature (anionic as 0.01 M SDS, cationic as 0.001 M CTAB, and 0.005 M TDAB, and non-ionic as 0.002 M Triton X100), at levels above their critical micellar concentrations, was also investigated. It was found that none of the surfactants produced any enhancement of the phosphorescence intensity. Conversely, the observed emission spectra from QDs solutions containing surfactants presented low signal to noise ratios (probably due to the formation of NPs aggregates resulting in undesirable light scattering and background).

From such experiments it can be concluded that the phosphorescence-like emission of Mn^{2+}-doped ZnS QDs is not significantly affected by typical parameters that usually modify the emission of traditional organic phosphors (e.g. pH, dissolved

oxygen, presence of heavy atoms or rigidity afforded by organized media). Such robustness of the delayed emission of Mn doped opens the way to simpler, more precise and more robust RTP analytical methodologies, as compared with conventional organic dyes-based existing RTP analytical methods.

3.1.5. Photostability

Several authors demonstrated that exposure of colloidal QDs, after their synthesis or further functionalization, to UV or visible light results in an important increase of the nanoparticles photoluminescence [35–37].

Such phenomenon, frequently known as photoactivation process, is aimed at removing of topological surface defects in the QDs eventually originated during the synthesis processes lowering the emitted luminescence [35–37]. Therefore, we have also evaluated the eventual effect of a photoactivation process on Mn^{2+}-doped ZnS QDs synthesized in our laboratory.

For this purpose, Mn:ZnS QDs were illuminated under a 290 nm source excitation for 2 h and no significant variation on the observed luminescence signal was noticeable. Again, the synthetic procedure here followed resulted in high-quality Mn:ZnS QDs, exhibiting a very stable phosphorescent signal at room temperature, without the need of previous photoactivation.

3.2. Effect of acetone on Mn:ZnS QDs phosphorescence

The study of the interaction of different chemical species with the surface of colloidal QDs, widely reported in the literature, has revealed that luminescence properties of these nanomaterials strongly depends on their surface atoms and their environment [9,38]. In this sense, previous research carried out in our laboratory has demonstrated the strong effect of the presence in the QDs environment of organic vapours [39], metallic cations [40] or inorganic anions [41] on the fluorescence emission of CdSe QDs. The mechanism proposed in each application depends on the reactive species (e.g. electrostatic interaction with the QDs surface ligands [29], electron transfer from conductive band of QD to unoccupied molecular orbital of the analyte [42], or a simple adsorption onto the surface of the semiconductor nanoparticles [43]). This was the basis of the recent increasing research activity on the development of novel optical sensors based on QDs probes [9].

Following this approach, and based on our experience with CdSe QDs, in this article Mn:ZnS QDs have been investigated for optical sensing of acetone based on a phosphorescence detection. For such purpose, Mn:ZnS QDs capped with L-cysteine were selected. The presence of L-cysteine on the QDs surface ensures water solubility of the nanoparticles. Moreover, terminal functional groups of the aminoacid might easily interact with acetone present in the medium, and, eventually, this interaction would affect to the luminescence of the QDs, which would be used to develop the acetone sensor aforementioned.

Thus, first studies were aimed to explore the behaviour of Mn^{2+}-doped ZnS QDs for phosphorescence detection-based acetone analysis. Spectroscopic measurements were performed in aqueous solutions buffered with SBB pH 12 as described in the general analytical procedure. The phosphorescence response of Mn^{2+}-doped ZnS QDs upon addition of increasing amounts of acetone, varying from 0.5 mg L^{-1} up to 600 mg L^{-1}, in aqueous solution is shown in Fig. 4. As it can be observed, the addition of acetone efficiently quenches the phosphorescence emission of the evaluated nanocrystal colloidal solution.

The dependence of the measured phosphorescent intensity signal with increasing concentrations of acetone was fitted to a Stern–Volmer equation. For this purpose, $(I_o/I)-1$ has been represented versus acetone concentration, where I_o is the phosphorescent emission of Mn:ZnS QDs without presence of acetone, and I is the phosphorescent emission of Mn:ZnS QDs in presence of increasing concentrations of acetone. The Stern–Volmer representation gives rise to a linear plot up to a concentration of at least 600 mg L^{-1} of acetone, which was the maximum concentration of analyte assayed. Such acetone quenching effect can be attributed to an interaction with the L-cysteine ligands present in the NPs surface, used to stabilize the QDs in aqueous solutions, as discussed in the next section.

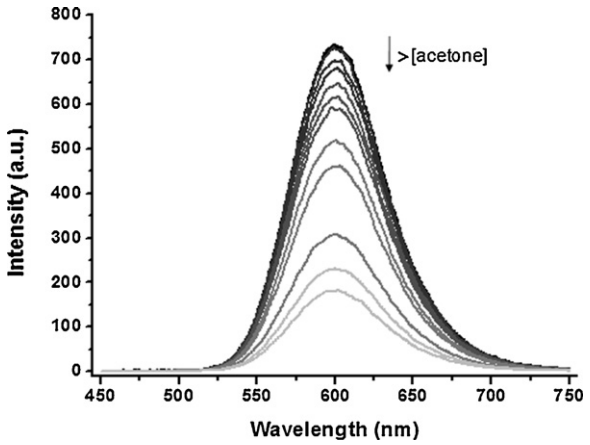

Fig. 4. Effect of the addition of acetone (from 0.5 mg L^{-1} up to 600 mg L^{-1}) on the phosphorescence emission of Mn:ZnS QDs.

4. Proposed mechanism

It is well known that acetone can act as an electrophile group. Therefore, there is a high probability of an interaction of the acetone with the amino group from the L-cysteine of the QDs, which is a nucleophile, to form an imine. Then, addition of more acetone to the medium could give rise to a further generation of an oxazolidone cycle. Based on its chemical structure, imine could act as an efficient electron acceptor. Therefore, such eventual chemical transformation of the L-cysteine in the presence of acetone would result in a quenching of the photoluminescence emission from the QDs probably due to an electron transfer process. Hence, if this occurs, changes on the surface charge of the QDs should be observed in the presence of acetone.

In order to confirm such possible quenching mechanism we carried out the measurement of the Z-potential of the QDs solution before and after the addition of acetone (see Fig. 6). When the Z-potential was measured in acidic medium (using acetic acid), a value of +24.4 mV was obtained (a positive value attributed to the protonation of the amino group of the L-cysteine). Conversely, this Z-potential decreases to a value around 0 mV when acetone is added to the QDs sample. This variation could be explained considering the loss of the positive charge from the amino group (see Fig. 5) when the imine or the oxazolidone are generated upon acetone addition.

Furthermore, the effect of different aliphatic and aromatic ketones, such as 2-heptanone and cyclohexanone, on the RTP emission from the QDs was also investigated. Results showed that such species produced also a significant quenching of the luminescence emission from the nanoparticles, thus probing the proposed imine formation between cysteine and the ketones.

4.1. Analytical performance characteristics

The analytical performance characteristics of the new RTP method were evaluated under the optimized experimental conditions. Calibration graphs were prepared from the results of

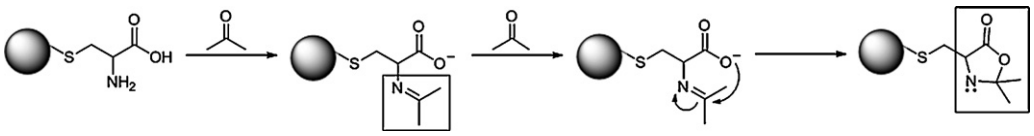

Fig. 5. Scheme of the proposed sensing mechanism.

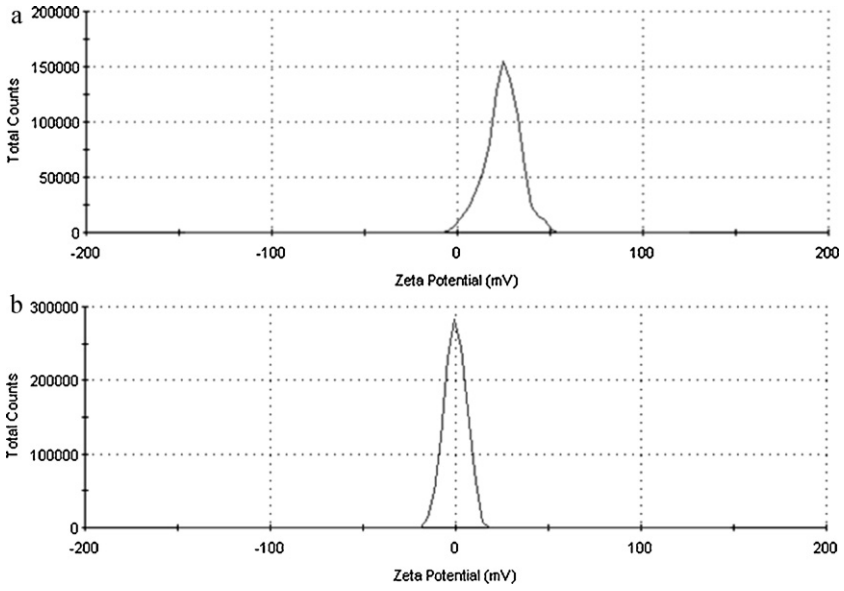

Fig. 6. Z-potential of a colloidal solution of Mn:ZnS QDs (a) in water media and (b) in the presence of acetone.

triplicate analysis of acetone standard water solutions of increasing concentration and proved to be linear at least up to 600 mg L^{-1} of acetone (maximum concentration assayed). The detection limit, calculated as the concentration of acetone which produced an analytical signal three times the standard deviation of 10 injections of a blank, turned out to be 0.2 mg L^{-1} of acetone. The precision of the proposed method was evaluated as the relative standard deviation of three replicates of a sample containing 15 mg L^{-1} of acetone and turned out to be ±2%.

The selectivity of the proposed methodology was assessed by studying the effect of the presence of different potential interferents on the QDs RTP signals. In this sense, it could be expected that the presence of metallic cations reacting with L-cysteine coating would alter the surface of the nanoparticles so changing the phosphorescent emission. Thus, emission of Mn:ZnS QDs was studied under increasing concentrations of some metal cations potentially present in environmental samples (using the optimized procedure previously described). The presence of Na(I), Eu(III), Zn(II) and Mn(II) up to 10 mg L^{-1} result in deviations of the fluorescence signal lower than 5%. However, the presence of Cu(II), Fe(III), Ag(I) or Hg(II) at a concentration level over 0.04 mg L^{-1} produced a change on the measured luminescence over 10% when working at acid or neutral pHs. In order to avoid such interferences, the same study was performed at a higher pH (pH 12). In such basic medium, it was observed that none of the assayed species produced any detectable interferent effect at concentrations below 1 mg L^{-1}.

Another type of compounds that could be present in polluted water samples includes different organic solvents, such as methanol, ethanol, 2-propanol, and acetonitrile. Results found showed again that none of such potential interferents assayed produced a detectable effect on the RTP emission of the QDs (even at the maximum concentration assayed of 5% (v/v).

As this methodology might be potentially applicable to RTP determination of acetone in urine samples, the effect of other components commonly present in urine at physiologically relevant levels was also evaluated. In this sense, histidine and L-cysteine were assayed at concentrations up to 1 mM, Na(I) up to 5 mM, K(I), Ca(II), Mg(II), D-glucose at concentrations up to 10 mM and finally urea—the main component of urine- up to 400 mM. As can be seen in Fig. 7, only L-cysteine and Ca(II) ion produced slight interference effects on the acetone signal. Moreover, it is worth noting that even high concentrations of glucose did not produce any noticeable change on the RTP of the QDs. This fact is particularly important for the eventual application of this RTP NPs-based methodology to the determination of acetone in patients suffering from Diabetes Mellitus.

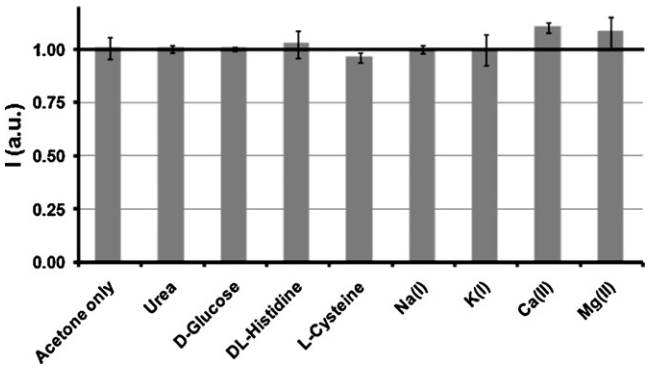

Fig. 7. Interference assay for acetone determination. 100 mg L^{-1} acetone was added in all cases, either alone or together with the potential chemical interferents assayed. Three replicates per point.

Table 1
Determination of acetone in enriched samples by using the phosphorescent QDs.

Type of sample	Acetone spiked ($mg\,L^{-1}$)	Acetone measured ($mg\,L^{-1}$)	Recovery (%)
Mineral water	6.3	6.8 ± 0.6	107
Tap water	9.5	9.3 ± 2.0	98
Sea water	8.2	8.6 ± 0.7	105
Matrix urine 1	24.9	25.5 ± 2.0	99
Matrix urine 2	73.9	76.9 ± 0.9	104
Matrix urine 3	98.9	91.1 ± 2.0	93
Urine 1	192.3	184.9 ± 1.2	96
Urine 2	535.7	547.9 ± 1.8	102

5. Real sample applications

The usefulness of the proposed method for the determination of acetone in natural water (tap, water, mineral and sea water) was first evaluated by following the general procedure. Water samples, spiked with known concentrations of acetone, were analyzed after filtration through 0.45 μm and 0.22 μm filter devices without any other sample pre-treatment. Then, 9 mL of the water samples were thoroughly mixed with 1 mL of Mn:ZnS QDs solution at pH 12 and the luminescence measurements were performed. Table 1 collects the results obtained after the analysis of trace levels of acetone in three different contaminated water samples.

Acetone determination in urine was also demonstrated at different acetone concentrations. The levels of acetone selected in order to carry out this study were on the same order of magnitude that those analyzed with commercial test strips. In a similar way to water samples analyses, urine samples were analyzed after filtration, and 1 mL of the urine samples were thoroughly mixed with 3 mL of Mn:ZnS QDs solution at pH 12. Unfortunately, results obtained for direct real urine samples analyses showed a deviation from values obtained with an external calibration. Thus, with the aim of avoiding such matrix effects, analysis of acetone in urine was carried out using a standard addition methodology. Luminescence measurements were performed and results obtained for the phosphorescent determination of acetone are collected in Table 1.

Good recoveries for the determination of acetone were obtained in all cases, thus indicating the validity of the proposed method for direct analysis of acetone in different types of water and urine samples.

6. Conclusions

In summary, Mn^{2+}-doped ZnS QDs exhibiting a strong and highly stable phosphorescence emission were successfully synthesized and exhaustively characterized. Several factors that have a strong influence over the classical phosphorescence emission do not modify the emission of the Mn:ZnS QDs, making this type of nanoparticles very robust for real sample applications. The nanoparticles have demonstrated a high selectivity for the acetone determination in aqueous media by measuring the phosphorescence quenching effect observed after analyte interaction with the colloidal nanoparticles. A possible mechanism was also proposed to explain the process of the acetone effect on the QDs phosphorescence.

Acknowledgements

This work was supported by the project CTQ-2006-02309 (Ministerio de Educacion y Ciencia, Spain). Emma Sotelo-Gonzalez acknowledges a grant (BP08-063) from Consejeria de Educacion y Ciencia of the Principado de Asturias. We thank to Nanotechnology and Electronic Microscopy and Microanalysis of SCTs of University of Oviedo for their help in nanoparticle characterization and Ainhoa Diaz-Pardo for their help.

References

[1] E. Zervas, X. Montagen, J. Lahaye, Atmos. Environ. 35 (2001) 1301–1306.
[2] A. Brega, P. Villa, G. Quadrini, A. Quadro, C. Lucarelli, J. Chromatogr. 553 (1991) 249–254.
[3] D.L. Giokas, G.Z. Tsogas, A.G. Vlessidis, Anal. Chim. Acta 651 (2009) 188–195.
[4] E.D. Hudson, K. Okuda, P.A. Ariya, Anal. Bioanal. Chem. 388 (2007) 1275–1282.
[5] G. Burini, R. Coli, Anal. Chim. Acta 511 (2004) 155–158.
[6] L. Dong, X. Shen, C. Deng, Anal. Chim. Acta 569 (2006) 91–96.
[7] P. Yang, C. Lau, X. Liu, J. Lu, Anal. Chem. 79 (2007) 8476–8485.
[8] R. Garrido-Delgado, L. Arce, C.C. Perez-Marin, M. Valcarcel, Talanta 78 (2009) 863–868.
[9] J.M. Costa-Fernandez, R. Pereiro, A. Sanz-Medel, Trends Anal. Chem. 25 (2006) 207–218.
[10] J. Riegler, T. Nann, Anal. Bioanal. Chem. 379 (2004) 913–919.
[11] M.F. Frasco, N. Chaniotakis, Anal. Bioanal. Chem. 396 (2010) 229–240.
[12] D.M. Willard, Anal. Bioanal. Chem. 376 (2003) 284–286.
[13] M. Bruchez, M. Moronne, P. Gin, S. Weiss, A.P. Alivisatos, Science 281 (1998) 2013–2016.
[14] A.M. Smith, S. Nie, Analyst 129 (2004) 672–677.
[15] U. Resch-Genger, M. Grabolle, S. Cavaliere-Jaricot, R. Nitschke, T. Nann, Nat. Methods 5 (2008) 763–775.
[16] S.G. Penn, L. He, M.J. Natan, Curr. Opin. Chem. Biol. 7 (2003) 609–615.
[17] D.E. Moore, K. Patel, Langmuir 17 (2001) 2541–2544.
[18] C.A.J. Lin, T. Liedl, R.A. Sperling, M.T. Fernandez-Argüelles, J.M. Costa-Fernandez, R. Pereiro, A. Sanz-Medel, W.H. Chang, W.J. Parak, J. Mater. Chem. 17 (2007) 1343–1346.
[19] H. Yang, S. Santra, P.H. Holloway, J. Nanosci. Nanotechnol. 5 (2005) 1364–1375.
[20] N.S. Karan, D.D. Sarma, R.M. Kadam, N. Pradhan, J. Phys. Chem. Lett. 1 (2010) 2863–2866.
[21] R. Beaulac, P.I. Archer, X. Liu, S. Lee, G.M. Salley, M. Dobrowolska, J.K. Furdyna, D.R. Gamelin, Nano Lett. 8 (2008) 1197–1201.
[22] R. Beaulac, P.I. Archer, D.R. Gamelin, J. Solid State Chem. 181 (2008) 1582–1589.
[23] M. Wang, L. Sun, X. Fu, C. Liao, C. Yan, Solid State Commun. 115 (2000) 493–496.
[24] A. Segura-Carretero, A. Salinas-Castillo, A. Fernández-Gutiérrez, Crit. Rev. Anal. Chem. 35 (2005) 3–14.
[25] Y. He, H.F. Wang, X.P. Yan, Anal. Chem. 80 (2008) 3832–3837.
[26] H.F. Wang, Y. Li, Y.-Y. Wu, Y. He, X.-P. Yan, Chem. Eur. J. 16 (2010) 12988–12994.
[27] P. Wu, Y. He, H.-F. Wang, X.-P. Yan, Anal. Chem. 82 (2010) 1427–1433.
[28] P. Wu, L.-N. Miau, H.-F. Wang, X.-G. Shao, X.-P. Yan, Angew. Chem. Int. Ed. 50 (2011) 8118–8121.
[29] J. Chen, A. Zheng, Y. Gao, C. He, G. Wu, Y. Chen, X. Kai, C. Zhu, Spectrochim. Acta A 69 (2008) 1044–1052.
[30] A.F.E. Hezingera, J. Tessmara, A. Göpferich, Eur. J. Pharm. Biopharm. 68 (2008) 138–152.
[31] B. Gammelgaard, O. Jons, J. Anal. At. Spectrom. 14 (1999) 867–874.
[32] A.A. Bol, A. Meijerink, J. Phys. Chem. B 105 (2001) 10197–10202.
[33] M.E. Diaz-Garcia, A. Sanz-Medel, Anal. Chem. 58 (1986) 1436–1440.
[34] T. Vo-Dinh, Room Temperature Phosphorimetry for Chemical Analysis, Wiley, New York, 1984.
[35] C. Carrillo-Carrion, S. Cardenas, B.M. Simonet, M. Valcarcel, Chem. Commun. 35 (2009) 5214–5226.
[36] C.T. Yuan, W.C. Chou, D.S. Chu, Y.N. Chen, C.A. Lin, W.H. Chang, Appl. Phys. Lett. 92 (2008) 183108–183111.
[37] M. Oda, J. Tsukamoto, A. Hasegawa, N. Iwami, K. Nishiura, I. Hagiwara, N. Ando, H. Horiuchi, T. Tani, J. Lumin. 122–123 (2007) 762–765.
[38] L. Qu, X. Peng, J. Am. Chem. Soc. 124 (2002) 2049–2055.
[39] M. Hasani, A.M. Coto-Garcia, J.M. Costa-Fernandez, A. Sanz-Medel, Sens. Actuators B: Chem. 144 (2010) 198–202.
[40] M.T. Fernandez-Argüelles, W.J. Jin, J.M. Costa-Fernandez, R. Pereiro, A. Sanz-Medel, Anal. Chim. Acta 549 (2005) 20–25.
[41] W.J. Jin, M.T. Fernandez-Argüelles, J.M. Costa-Fernandez, R. Pereiro, A. Sanz-Medel, Chem. Commun. (2005) 883–885.
[42] R. Tu, B. Liu, Z. Wang, D. Gao, F. Wang, Q. Fang, Z. Zhang, Anal. Chem. 80 (2008) 3458–3465.
[43] A.V. Isarov, J. Chrysochoos, Langmuir 13 (1997) 3142–3149.